RHEOLOGICAL CALCULATIONS OF CONCENTRATED SUSPENSIONS BASED ON THE NEW THEORY

by Kaichi Izumi*, and Kenichi Hattori**

*Research and Developement Section, Kao Corporation
1 − 3, 2 − chome, Bunka, Sumida − ku, Tokyo, 131, JAPAN

**Department of Civil Engineering,
Faculty of Science and Technology, Chuo University
13 − 17, 1 − chome, Kasuga, Bunkyo − ku, Tokyo, 112, JAPAN

1. Theoretical background

1.1 Viscosity theory

About three centuries have passed after Newton[1], in his famous "PRINCIPIA", has defined viscosity. It has been about 150 years since Hagen[2] and Poiseuille[3] have discovered independently the (capillary) method of determining the viscosity. Before their discovery, the viscosity was merely a definition of the fluid property and the difference between Newtonian and non–Newtonian viscosity was not known. After the measurement of viscosity became possible, the exsistence of fluids the flow property of which was not conforming to the Newton's flow equation (1) became to be known.

$$\tau = \eta \cdot \gamma \qquad \cdots\cdots\cdots\cdots\cdots\cdots\cdots\cdots\cdots\cdots\cdots\cdots\cdots\cdots\cdots\cdots\cdots\cdots\cdots\cdots\cdots\cdots(1)$$

τ : shear stress
η : viscosity
γ : shear rate

Currently, three types of flow as illustrated in FIG. 1 are known. The line **A** in FIG. 1 describes the Newtonian flow the shear stress of which is proportional to the shear rate. Curves **B** and **C** describe the non–Newtonian flow. Curve **B** is frequently observable for suspensions such as cement pastes and other mixtures of solid particles and liquids, and curvre **C** for polymer solutions such as multi grade engine oils. Although the curve **B** is shown for representing the non–Newtonian flow of a suspension, the shape of which varies widely according to the conditions of experiment to draw a flow curve as shown in FIG. 2.

Due to variation of the shape of flow curves, it is meaningless to classify non–Newtonian fluids as substances by the shape although it is not meaningless to classify the flow phenomena. There are non–Newtonian flow equations proposed by Bingham[4, 5], Harschel and Bulkley[6, 7], and by Casson[8] but none of the non–Newtonian curves in FIGs. 1 and 2 are expressible by these equations.

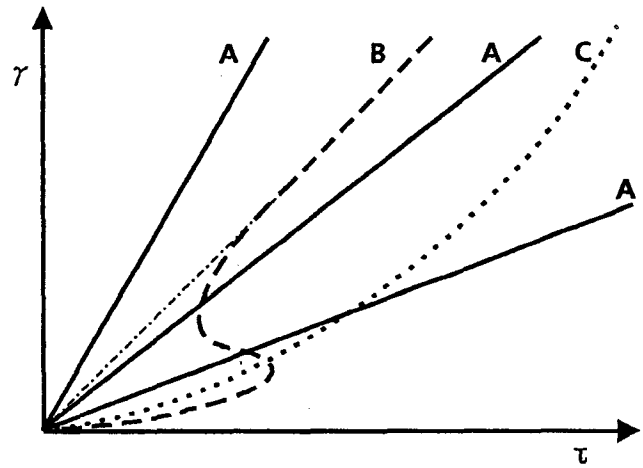

FIGURE 1. Three Types of Flow

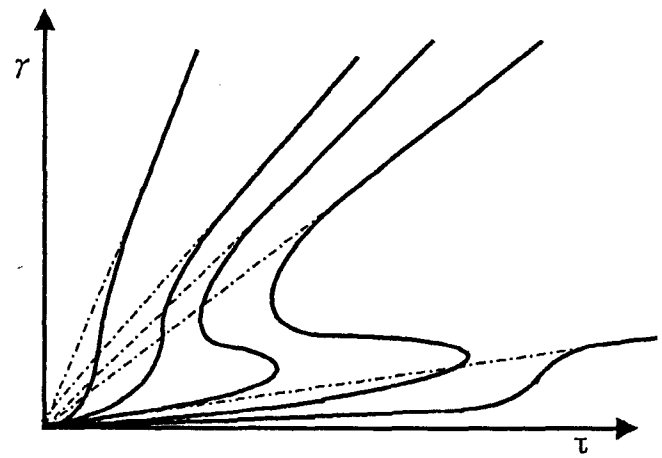

FIGURE 2. Variation of Flow Curve of Suspension

The reason why these equations are not capable of expressing the popularly known non–Newtonian flow curves may be attributable to the fact that non–Newtonian viscosity in these equations has not been properly defined. The term "apparent viscosity" have been used to discriminate non–Newtonian viscosity from Newtonian viscosity without an interpretation on the mechanism of resistance against the flow.

As another approach to establish a non–Newtonian viscosity theory, modifications of the famous Einstein equation (2)[9, 10] have been tried frequently.

n_1 : number of liquid molecules in unit volume
n_2 : number of primary particles in unit volume
n_3 : number of primary particles in unit volume
$U = J/n$, J : number of junctions between constituents

It is generally known that liquid molecules are in random thermal motion and not all of them are making contact with each other, but due to the huge number ($10^{16 \sim 18}$) in unit volume and to the very rapid motion, the variation in number of friction points or of junctions is not observable.

If we assume that the total surface area of particles is constant regardless of the state of coagulation of particles, the number of friction points between particles and liquid molecules is considered constant, and by the above explained reasons, we may assume that U_1 and U_2 are constant (equal to 1). The constant viscosity of a Newtonian liquid or of a suspension in the state of complete dispersion is thus explainable by the constancy of number of junctions.

Due to the large mass and to the large quantity of motion of particles in suspension, the velocity of motion is much slower and the frequency of collision is much lower as compared to those of the liquid molecules, and the variation of number of junctions between particles is observable. The variable (non–Newtonian) viscosity is explainable by the variation of number of junctions.

The expression of eq. (4) seems more reasonable than that of eq. (2) since it contains the terms describing both the properties of liquid (B_1) and the particle (B_2). As is well known, Einstein, when he proposed eq. (2)[9, 10], considered a system of complete dispersion (without an interaction between particles). If a suspension is in the state of complete dispersion, then there is no point of friction between particles ($U_3 = 0$), and eq. (4) expresses the constsnt (Newtonian) viscosity.

There is a problem when one tries to use Einstein equation (or eq. (4) without the third term in the right side) because it is very difficult (practically impossible in some cases) to confirm that the sample suspension is in the state of complete dispersion. Without this confirmation, there is no reason to justify the application of Einstein equation to a suspension.

It is also well known that the difference bretween calculated viscosities by eq. (2) and measured viscosities becomes larger for the suspensions of higher particle concentrations. This seems very natural because Einstein equation neglects the particle–particle interaction the probability of which increases as the particles concentration increases.

As eq. (3) was extended to express both the Newtonian and non–Newtonian viscosities, Newton's flow equation (1) was extended to express both the Newtonian and non–Newtonian flow curves (eq. (5)) correspondingly.

$$\tau = \eta_s \cdot \gamma = \gamma \cdot \{B_1 \cdot (n_1 \cdot U_1)^{2/3} + B_2 \cdot (n_2 \cdot U_2)^{2/3} + B_3 \cdot (n_3 \cdot U_3)^{2/3}\} \quad \cdots\cdots (5)$$

$$\eta_s = \eta_m \cdot (1 + 2.5 \cdot Cv) \quad \ldots\ldots\ldots\ldots\ldots\ldots\ldots\ldots (2)$$

η_s : viscosity of suspension
η_m : viscosity of medium
Cv : volume concentration (fraction) of particle

Although over hundred modifications of eq. (2) have been proposed[11 ~ 13], this approach has not been successful and the reason of this may be attributable to the problems associated with the original equation. Since eq. (2) does neither contain the terms describing the time–dependency and the shear–dependency of viscosity nor the term for representing the specific property of particles, this equation is considered to be not suitable as a fundamental equation describing the non–Newtonian viscosity.

Other than the approaches mentioned as above, there have been works[14 ~ 29] in efforts to establish non–Newtonian viscosity equation based on the destruction of coagulated structure or the decreasing number of junctions between particles. One of the serious problems associated with this approach may be a lack of an appropriate consideration on the increasing number of junctions between particles caused by the naturally ocurring coagulation.

As a solution for the lack of proper terms or the definition of non–Newtonian viscosity, the authors[30 ~ 37] considered an application of classical concept in which the viscosity was attributed to the friction between the constituents of a fluid. By introducing the concept of friction, the viscosity (η) of a Newtonian liquid is expressed as follows;

$$\eta = B \cdot n^{2/3} \quad \ldots\ldots\ldots\ldots\ldots\ldots\ldots\ldots\ldots\ldots\ldots\ldots (3)$$

B : coefficient of friction as expressed in units of dyn·sec between two liquid molecules
n : number of liquid molecules in unit volume

If we apply the same concept of friction to a suspension consisting of a kind of particle and a liquid, and introducing the term U which denotes the ratio between the number of friction points or the number of junctions J and the number of conponents n, eq. (3) is extended to express the viscosity of a mixture as follows;

$$\eta_s = \eta_1 + \eta_2 + \eta_3$$
$$= B_1 \cdot (n_1 \cdot U_1)^{2/3} + B_2 \cdot (n_2 \cdot U_2)^{2/3} + B_3 \cdot (n_3 \cdot U_3)^{2/3} \quad \ldots\ldots\ldots (4)$$

η_1 : viscosity originating from friction between liquid molecules
η_2 : viscosity originating from friction between particles and liquid moleclues
η_3 : viscosity originating from friction between particles

B_1 : coefficient of friction between two liquid molecules
B_2 : coefficient of friction between a particle and all liquid molecules surrounding it
B_3 : coefficient of friction between two particles

1.2 States of dispersion and coagulation

As U_3 is an only variable in the right side of eq. (4), an equation describing a varying viscosity of a suspension is considered to be obtainable if the practical form of equation expressing U_3 is known. For obtaining the equation expressing the variation of number of junctions, the authors considered an application of the coagulation rate theory established by Verwey and Overbeek[38]. Since the chain structure of coagulated particles is assumed in the Verwey–Overbeek theory, the authors examined the pertinence of applying this theory to the concept of junction viscosity. When the chain structure of coagulation is assumed, all the particles in the system has to form a chain at the state of complete coagulation theoretically, and the resulting system may not be homogeneous. This may restrict an applicability of the author's theory of junction viscosity to an exsisting system since the homogeniety to a certain extent (at least macroscopically) is necessary for claiming that the viscosity calculated based on the theory represents the viscosity of the whole system.

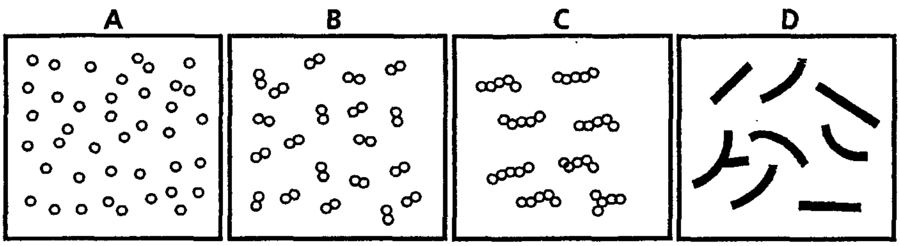

	A	B	C	D
degree of dispersion	1.00	0.50	0.20	0.01
degree of coagulation	0	0.50	0.80	0.99

Each chain consists of 100 primary particles

FIGURE 3. States of Dispersion and Coagulation

A system containing a chain of particles is evidently unhomogeneous and the viscosities of parts with and without the chain are entirely different, but considering the process of coagulation starting from the completely dispersed state, it is possible to assume that the coagulation progresses from A to D as shown in FIG. 3. Since $10^9 \sim 10^{12}$ particles are contained in a concentrated suspension, $10^7 \sim 10^{10}$ coagulated particles (n_t) are present in unit volume at 99 % coagulation if we define the degrees of dispersion (D_d) and of coagulation (D_c) as follows;

$$\left.\begin{aligned} D_d &= n_t / n_3 \\ D_c &= 1 - D_d \end{aligned}\right\} \qquad \cdots\cdots (6)$$

Even at 99.9 % coagulation, there still are $10^6 \sim 10^9$ coagulated particles and this particle number is considered to be large enough to ensure the homogeniety of a sample suspension subjected to rheological measurements. Based on the reasons mentioned as above, the authors judged that the coagulation rate theory and the junction viscosity theory assuming the chain structure of coagulation are applicable for the calculations of junction number and the viscosity of concentrated suspensions.

2. Derivation of viscosity equations

2.1 Equations for the calculation of junction number

According to Verwey–Overbeek theory[38], the interaction potential energy of charged particles in a suspension is expressed as follows;

$$V = V_R + V_A$$

$$= \frac{\varepsilon \cdot \phi^2 \cdot r}{2} \cdot \ell n(1 + e^{-\kappa D}) - \frac{A}{6}\left\{\frac{2}{S^2} + \frac{2}{(S^2-4)} + \ell n \frac{(S^2-4)}{S^2}\right\} \quad \cdots\cdots(7)$$

$$S = 2 + D/r$$

where,

V	:	Interaction potential energy
V_R	:	Repulsive potential energy
V_A	:	Attractive potential energy
r	:	Radius of particle
ε	:	Dielectric constant of medium
ϕ	:	Surface charge of particles
D	:	Surface-surface distance between particles
A	:	Hamaker's attraction constant
κ	:	Debye-Hückel parameter

$$\kappa = \sqrt{\frac{8 \cdot \pi \cdot N \cdot I}{1000 \cdot \varepsilon \cdot k \cdot T}} \cdot E$$

From the same theory, the rate of coagulation or the decreasing number of particles is expressed as follows;

$$-\frac{dn_t}{dt} = 2 \cdot K \cdot \kappa \cdot r \cdot n_t^2 \cdot e^{-V_{max}/kT} \quad \cdots\cdots(8)$$

V_{max}	:	Maximum interaction potential energy
n_3	:	Primary particle number
n_t	:	Particle number at a given time t
K	:	Smoluchowski's rapid coagulation rate constant $K = 4 \cdot k \cdot T / 3 \cdot \eta_m$
η_m	:	Viscosity of medium
k	:	Boltzmann constant
T	:	Temperature in °K
E	:	Unit charge
N	:	Avogadro number
I	:	Ion concentration, N/ℓ

Eq. (8) integrates to,

$$\frac{1}{n_t} - \frac{1}{n_3} = 2 \cdot K \cdot \kappa \cdot r \cdot t / e^{V_{max}/kT} \quad \cdots\cdots(9)$$

and from eq. (9), we have,

$$n_t = \frac{n_3 \cdot e^x}{Pt + e^x} \quad \cdots\cdots\cdots\cdots (10)$$

by writing $P = 2 \cdot K \cdot \kappa \cdot r \cdot n_3$, and $x = V_{max} / kT$.

Since the number of junctions at a given time J_t for the chain structure is,

$$J_t = n_3 - n_t \quad \cdots\cdots\cdots\cdots (11)$$

we have,

$$J_t = \frac{n_3 \cdot Pt}{Pt + e^x} \quad \text{or} \quad \frac{J_t}{n_3} = U_3 = \frac{Pt}{Pt + e^x} \quad \cdots\cdots\cdots (12)$$

Eq. (12) is further simplified by writing $H = P / e^x$ as follows;

$$U_3 = \frac{Ht}{Ht + 1} \quad \cdots\cdots\cdots\cdots (13)$$

As U_3 is equal to 1/2 at the half life time of the particle number t_H,

$$\frac{Ht_H}{Ht_H + 1} = \frac{1}{2} \quad \rightarrow\rightarrow\rightarrow\rightarrow \quad H = \frac{1}{t_H} \quad \cdots\cdots\cdots\cdots (14)$$

From eq.(14), we may name H the coagulation rate constant because its physical dimension is $[T^{-1}]$ which is the same as those of many rate constants. It is the only parameter expressing the rate of coagulation in eq. (13) and in the viscosity equations in the present theory which will be shown later.

For the cement paste of any water/cement ratio R, the volume fraction of particle Cv is calculable as follows;

$$Cv = \frac{\rho_1}{\rho_1 + \rho_2 \cdot R} \quad \cdots\cdots\cdots\cdots (15)$$

where ρ_1 is the specific gravity of the medium and ρ_2 is that of the particle. The (average) radius of particle r is calculable from the specific surface σ as follows;

$$r = \frac{3}{\rho_2 \cdot \sigma} \quad \cdots\cdots\cdots\cdots (16)$$

and from R and Cv, the primary particle number n_3 is calculable as follows.

$$n_3 = \frac{3 \cdot Cv}{4 \cdot \pi \cdot r^3} \quad \cdots\cdots\cdots\cdots (17)$$

As described previously, the coagulation rate constant H is equal to P / e^x having the dimension $[T^{-1}]$. If we analyze the dimensions of parameters in eq. (8) ~ (13), we would find that H, P, and x contain the values having the dimension corresponding to the unit erg/erg which may be called a dimensionless energy. In unagitated suspensions, the particles tend to coagulate to reduce the internal energy expressed by P in the dimensionless form. If

the repulsive potential energy V_R is large, it reduces the rate of coagulation by making the value of dimensionless energy P/e^x or H small.

It seems reasonable to consider that low (dimensionless) energy states of dispersion correspond to high viscosity and high energy states to low viscosity. This consideration fits well with the viscosity decrease of agitated suspensions because the energy in suspensions increases with mechanical agitation.

The expression of dimensionless energy for representing the shear rate is directly obtainable from the dimensional analysis of Newton's flow equation (1) as follows;

$$\gamma = \frac{\tau\,(\mathrm{dyn/cm^2})}{\eta\,(\mathrm{dyn\cdot sec/cm^2})} = \frac{\tau\,(\mathrm{dyn\cdot cm/cm^3})}{\eta\,(\mathrm{dyn\cdot cm\cdot sec/cm^3})} = \frac{\tau\,(\mathrm{erg})}{\eta\,(\mathrm{erg\cdot sec})} \quad \cdots\cdots(18)$$

The same expression is obtainable by denoting the total mechanical energy (of agitation) E_m put into the system (of viscosity measurement) during the period of time t and dividing it by kT to be the same as the expressions for energy in the coagulation rate theory.

$$\gamma = \frac{E_m}{kTt} \quad \text{or} \quad \gamma t = \frac{E_m}{kT} \quad \cdots\cdots(19)$$

As far as the authors could find in the literature, the same expression (γt) was first used by Tattersall[39,40] for describing the decreasing viscosity of cement pastes. But unfortunately, his paper with its excellent suggestion has not attracted much attention from rheologists.

As the state of dispersion is described by the relationship between the potential energy and the relative distance between particles by eq. (7), it may be considered that the coagulation progresses by consuming the internal energy corresponding to Ht as expressed by eq. (13). To satisfy the law of conservation of energy and to maintain the relationship between the internal energy and the state of dispersion, the original state before consuming the internal energy corresponding to $H\cdot t$ must be recovered if the same amount of energy $\gamma\cdot t'\,(= H\cdot t)$ is supplied to the system from outside. For this reason, the expression for the influence of energy of agitation on the particle number is obtainable by back–tracing the curve expressed by eqs. (8) or (13).

For back–tracing the curve expressed by eq. (13), the relationship between the internal energy consumption and the external energy to recover the original state ($H\cdot t = \gamma\cdot t'$) must be modified as follows;

$$H\cdot t = 1/\gamma\cdot t \quad (H = 1/\gamma\cdot t^2) \quad \cdots\cdots(20)$$

By reversing the time axis and by introducing the relationship of eq. (20) into eq. (8), we have,

$$\frac{dn_t}{dt} = \frac{n_t^2}{n_3 \cdot \gamma \cdot t^2} \qquad \cdots\cdots(21)$$

which integrates to,

$$n_t = \frac{n_3 \cdot \gamma \cdot t}{\gamma \cdot t + 1} \qquad \cdots\cdots(22)$$

for the initial conditions $t = \infty$ and $n_t = n_3$. From eq. (22), we have the following (23) for expressing the influence of agitation in promoting the dispersion.

$$J_t = \frac{n_3}{\gamma \cdot t + 1} \quad \text{or} \quad \frac{J_t}{n_3} = U = \frac{1}{\gamma \cdot t + 1} \qquad \cdots\cdots(23)$$

Although eq. (23) expresses the rate of mechanical dissociation of the coagulated particles, it is not useful for the calculation of decreasing viscosity of actual suspension because the parameter γ only desacribes the mechanical dissociation rate. In the suspensions under the influence of the coagulation rate H, the natural coagulation of particles always progresses until the complete coagulation is reached, so, it is always necessary to have the parameter H in the equations to calculate the time-dependent viscosity.

2.2 Equations for the calculation of viscosity

For the suspensions, two initial states, the initially dispersed state and the initially coagulated state may be defined. For an initially dispersed suspension left unagitated, the coagulation progresses and the junction number increases according to eq. (12) or (13). If all the particles in suspension are completely dispersed, there is no junction to be destroyed by the agitation, but considering the process of preparing a suspension, the probability of finding or observing the completely dispersed state seems very low.

In many cases, the suspensions are prepared by mixing the particles (or powders) and the medium, and the particles before adding the medium is considered to be forming a coagulated structure of the higher order, in which the number of junctions is larger than the number of particles forming a simple chain. By the mixing at the preparation of suspension, the number of junction decreases to less than the number of particles, but as shown by eq. (23), it is not possible to attain the state of complete dispersion since it is not possible to make γ or t infinitively large. For this reason, suspension samples are not usually in the state of complete coagulation nor in that of the complete dispersion at the begining of viscosity measurements.

Although the states of complete dispersion or complete coagulation is not practically observable, we may define the theoretical time axis in which the suspensions initially have to be either in the state of complete coagulation in which J_t is equal to n_3 and n_t is equal to 0 or in the state of complete dispersion ($J_t = 0$, $n_t = n_3$).

For the chain structure of coagulation of particles, the following relationship between the particle number and the junction number is satisfied.

$$J_0 + n_0 = n_3, \qquad U_0 = J_0 / n_3 \ (= D_c \text{ at } t = 0)$$
$$J_t + n_t = n_3, \qquad U_3 = J_t / n_3$$
$$J_E + n_E = n_3, \qquad U_E = J_E / n_3 \ (= D_c \text{ at } t = t_E)$$

J_0 ; Junction number at the start of observation (experiments).
J_t ; Junction number at the experimental time t.
J_E ; Junction number at the time of equilibrium (explained later).

n_0 ; Particle number at the start of observation (experiments).
n_t ; Particle number at the experimental time t.
n_E ; Particle number at the time of equilibrium (explained later).

Since theoretical initial conditions of suspensions are not usually observable, it is important to note that almost all experimental data are described or illustrated on the experimental time axsis. The following FIG. 4 illustrates the difference between the theoretical time and the experimental time in which the observable viscosity changes are shown by solid lines.

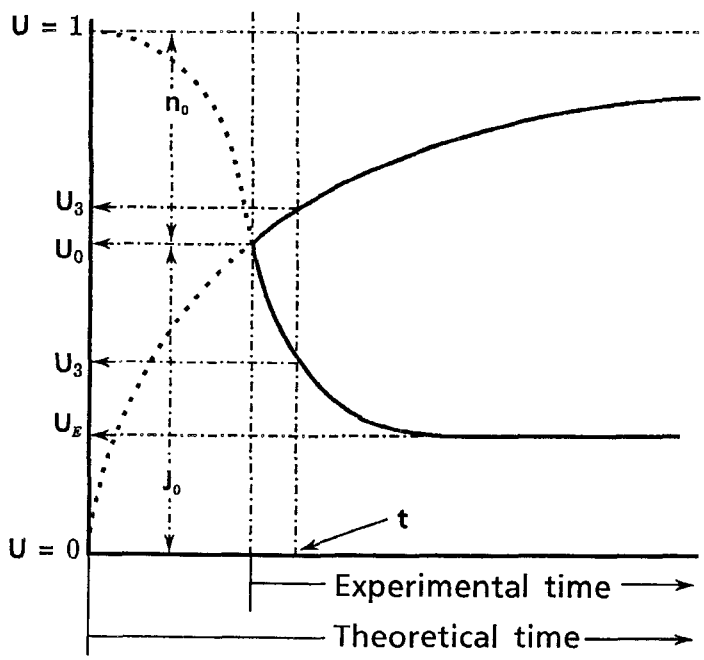

FIGURE 4. DEFINITION of TIME AXSIS

For the n_0 particles, the coagulation progresses at the rate of $Ht / (Ht + 1)$, but by the agitation (of rotor of the viscometer used for the measurement), the rate is reduced by the ratio corresponding to $1 / (\gamma t + 1)$. Consequently, the number of junction J_1 for n_0 particles at the time t is;

$$J_1 = \frac{n_0 \cdot Ht}{(Ht + 1)(\gamma t + 1)} \qquad \cdots\cdots(24)$$

For the J_0 junctions, the dissociation progresses at the rate $1 / (\gamma t + 1)$, and for the released particles by the dissociation $1 - (1 / (\gamma t + 1))$, the coagulation p rogresses at the rate $Ht / (Ht + 1)$. So the junction number J_2 originating from J_0 junctions at the time t is,

$$J_2 = \frac{J_0}{\gamma t + 1} + \frac{J_0 \cdot \gamma \cdot Ht^2}{(Ht + 1)(\gamma t + 1)}$$

$$= J_0 \cdot \{1 - \frac{\gamma t}{(Ht + 1)(\gamma t + 1)}\} \qquad \cdots\cdots(25)$$

Since the junction number at the time t is the sum of J_1 and J_2,

$$J_t = J_0 \{1 - \frac{\gamma t}{(Ht + 1)(\gamma t + 1)}\} + \frac{n_0 \cdot Ht}{(Ht + 1)(\gamma t + 1)}$$

$$= \frac{J_0 \cdot (\gamma Ht^2 + 1) + n_3 \cdot Ht}{(Ht + 1)(\gamma t + 1)} = n_3 \cdot \frac{U_0 \cdot (\gamma Ht^2 + 1) + Ht}{(Ht + 1)(\gamma t + 1)}$$

$$\cdots\cdots(26)$$

By substituting the initial condition for the initially coagulated suspension ($U_0 = 1$) into eq. (26), we have,

$$J_t = n_3 \{1 - \frac{\gamma t}{(Ht + 1)(\gamma t + 1)}\} \qquad \cdots\cdots(27)$$

and for the initially dispersed suspension ($U_0 = 0$), we have,

$$J_t = \frac{n_3 \cdot Ht}{(Ht + 1)(\gamma t + 1)} \qquad \cdots\cdots(28)$$

As the coagulation progresses, the number of isolated particles diminishes reducing the probability of collision between particles. As the dissociation of coagulated particles progresses, the rate of coagulation increases due to the increased number of particles and to the increased probability of collision. For this reason, there exists a time of equilibrium t_E at which the rates of coagulation and of mechanical dissociation become equal. After the time of equilibrium, the number of junctions remains constant. The time of equilibrium is calculable from the condition to make the derivatives of eqs. (26) ~ (28) equal to zero.

The derivative of eq. (26) is,

$$\frac{dJ_t}{dt} = n_3 \cdot [\frac{(\gamma Ht^2 - 1)\{U_0 \cdot (\gamma + H) - H\}}{(Ht + 1)^2 (\gamma t + 1)^2}] \qquad \cdots\cdots(29)$$

of eq. (27) is,

$$\frac{dJ_t}{dt} = \frac{n_3 \cdot \gamma \cdot (\gamma Ht^2 - 1)}{(Ht + 1)^2 (\gamma t + 1)^2} \qquad \cdots\cdots(30)$$

and of eq. (28) is,

$$\frac{dJ_t}{dt} = \frac{-n_3 \cdot H \cdot (\gamma H t^2 - 1)}{(Ht + 1)^2 (\gamma t + 1)^2} \qquad \cdots\cdots\cdots\cdots\cdots\cdots (31)$$

and the time of equilibrium is,

$$t_E^2 = \frac{1}{\gamma \cdot H} \qquad \text{or} \qquad t_E = \frac{1}{\sqrt{\gamma \cdot H}} \qquad \cdots\cdots\cdots\cdots\cdots (32)$$

As the equations (27) and (28) were obtained by substituting the initial conditions into eq. (26), the experimental time and the theoretical time are the same for eqs. (27), (28), (30), and (31). As $(\gamma H t^2)$ is always smaller than 1 initially (because $t = 0$), dJ_t/dt is initially negative by eq. (30), and by eq. (27), the viscosity decreases until the equilibrium between the coagulation rate and the mechanical dissociation rate is reached. For the same reason, the viscosity increases by eq. (28) until the equilibrium is reached.

The initial increase or the decrease of viscosity by the general viscosity equation (26) depends on both $(\gamma H t^2)$ and $H/(\gamma + H)$. When U_0 is larger than $H/(\gamma + H)$, the viscosity initially decreases since $(\gamma H t^2)$ is usually very small when t is nearly 0. The viscosity in this case decreases until the the time of equilibrium and remains constant afterwards. If U_0 is smaller than $H/(\gamma + H)$, the viscosity increases until the equilibrium is reached.

The number of junctions J_E at the time of equilibrium is calculable by substituting t_E into eqs. (26) ~ (28), and correspondingly we have,

$$J_E = n_3 \cdot \left\{ \frac{2 \cdot U_0 \cdot \sqrt{\gamma \cdot H} + H}{(\sqrt{H} + \sqrt{\gamma})^2} \right\} \qquad \cdots\cdots\cdots\cdots\cdots\cdots\cdots (33)$$

$$J_E = n_3 \cdot \left\{ 1 - \frac{\gamma}{(\sqrt{H} + \sqrt{\gamma})^2} \right\} \qquad \cdots\cdots\cdots\cdots\cdots\cdots\cdots (34)$$

$$J_E = \frac{n_3 \cdot H}{(\sqrt{H} + \sqrt{\gamma})^2} \qquad \cdots\cdots\cdots\cdots\cdots\cdots\cdots\cdots (35)$$

After obtaining the equations for the calculation of junction numbers J_t and J_E, the viscosity of a suspension originating from the particle–particle friction becomes calculable as follows based on eq. (4).

$$\left.\begin{aligned} \eta_3 &= B_3 \cdot J_t^{\,2/3} \\ \eta_E &= B_3 \cdot J_E^{\,2/3} \end{aligned}\right\} \qquad \cdots\cdots\cdots\cdots\cdots\cdots\cdots\cdots (36)$$

3. Calculations of viscosity

3.1 Equations expressing shear rates

As described previously, the viscosity originating from the particle–particle friction is expressed by eq. (26) which contain parameters B_3, n_3, H, γ, and U_0. Among these parameters, the method of calculation of n_3 was already shown by eqs. (15) ~ (17). Since the shear rate is an artificially subjective condition decided by the person who conducts the rheological experiments, any equation such as the following describing the time–shear rate relationship may be written.

$$\gamma = G \qquad \cdots\cdots (37.1)$$

$$\left.\begin{aligned} \gamma_1 &= G_1 \\ \gamma_2 &= G_2 \\ \gamma_3 &= G_3 \\ &\cdots\cdots \\ &\cdots\cdots \\ &\cdots\cdots \\ \gamma_n &= G_n \end{aligned}\right\} \cdots\cdots (37.2)$$

$$\gamma = G \cdot t \qquad \cdots\cdots (37.3)$$
$$\gamma = G \cdot t^{\alpha} \qquad \cdots\cdots (37.4)$$
$$\gamma = G \cdot (T - t) \qquad \cdots\cdots (37.5)$$
$$\gamma = G \cdot (T - t)^{\alpha} \qquad \cdots\cdots (37.6)$$
$$\gamma = G \cdot sin(\omega t + \alpha) \qquad \cdots\cdots (37.7)$$
$$\gamma = log\, G \cdot t \qquad \cdots\cdots (37.8)$$
$$\gamma = G \cdot e^{\alpha t} \qquad \cdots\cdots (37.9)$$

G, α, ω : dimensionless constants

Note : Eqs. (37.1) ~ (37.9) merely express the numerical relationship between the time and the shear rate. The dimensions of both sides of all equations are $[T^{-1}]$.

Eq. (37.1) describe the constant shear rate and (37.2) the stepwise change of shear rate. These equations are not useful for the calculation of flow curves and hysteresis loops although the conditions described by these equations are most frequently encountered in experiments and in industrial practices of handling the suspensions.

Eqs. (37.3) ~ (37.9) describes the continuous change of shear rate. Among the conditions described by eqs. (37.3) ~ (37.9), the linear change of shear rate (37.3) is considered to have been most frequently employed to draw flow curves although the influence of shear rate on the shear stress has not been known quantitatively. The authors have not seen a case in which the conditions described by eqs. (37.4) ~ (37.9) have been employed in the papers presented in the past to calculate the flow curves. Eq. (37.4) is considered to be useful in the investigation and the estimation of starting torque of agitators and (37.5) is necessary for the calculation of down curves of hysteresis loops. Other equations may be found to be of some practical use in future, but currently, these are practically useless.

3.2 Viscosity under constsnt shear rate

After defining the shearing (experimental) condition, the viscosity η_3 is calculable by eqs. (26) ~ (28) although B_3, H, and U_0 have to be known. Before showing the methods of calculation of these parameters, the viscosities of agitated and unagitated suspensions for the given values of;

$$r = 3\,\mu m$$
$$n_3 = 9 \times 10^9$$
$$B_3 = 6 \times 10^{-6}$$

were calculated to illustrate influences of the shear rate γ and the coagulation rate H,.

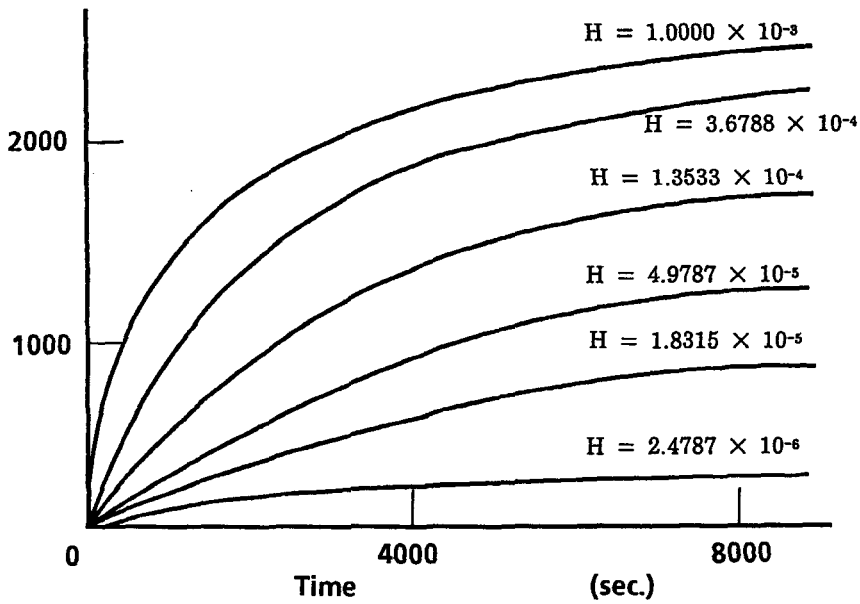

FIGURE 5. Time – Dependent Viscosity of Unagitated Suspension ($\gamma = 0$)[41]

Although the suspensions are not usually in the state of complete dispersion nor in that of the complete coagulation as mentioned previously, it is possible to assume that the same shear rate is mainteind all through the viscosity measurement (from the theoretical t = 0) if the constant shear rate (including $\gamma = 0$) is being employed. This assumption of constant shaer rate (including the periods before the observation) is important for the calculations of specific constants (B_3, H, and U_0) of each suspension sample and for the conversion of time axes (theoretical and experimental) which will be described later.

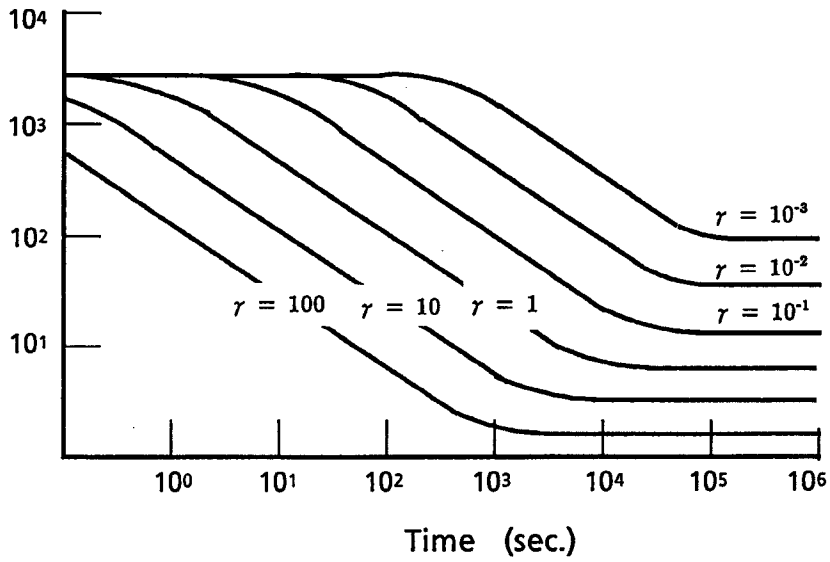

FIGURE 6. Time – Dependent Viscosity of Agitated Suspension (γ = 100 sec^{-1})[41]

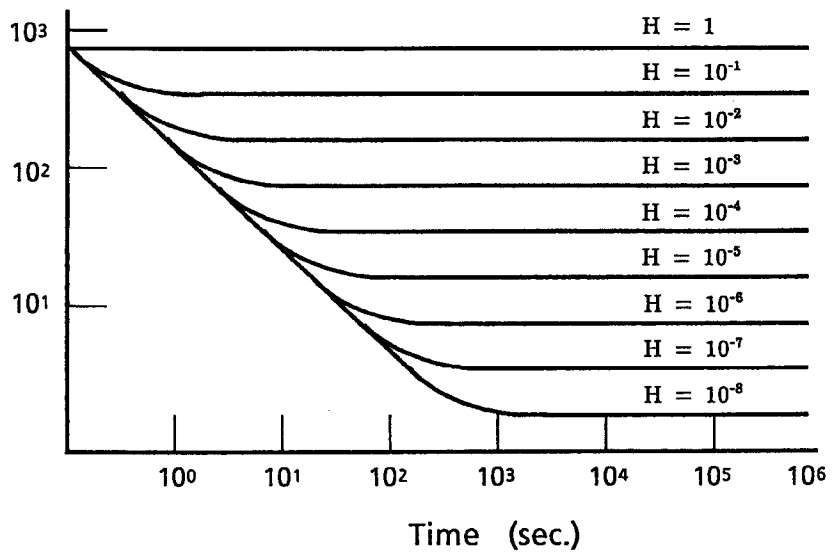

FIGURE 7. Time – Dependent Viscosity of Agitated Suspension (H = 10^{-8} sec^{-1})[41]

As shown by the FIG. 5, the viscosity of unagitated suspension is influenced by the coagulation rate constant H which may be modified by the addition of dispersant or coagulant. The coagulation rate is also modified by changing the viscosity of the medium

because H is equal to $(2 \cdot K \cdot \kappa \cdot r \cdot n_3 / e^x)$ and K (Smoluchowski's rapid coagulation rate constant) is inversely proportional to η_m (refer to page 6).

In FIG. 6, a so called shear thinning effect which has been explained by the destruction of coagulated structure of particles in the structural viscosity theory[14~29] appeared very clearly. Although the viscosity increase of an unagitated suspension and the viscosity decrease by the agitation have been popularly known as phenomena, there has been no reliable theory explaining the relationship between the changing viscosity and the values of H and γ, but by FIGs. 5 ~ 7 which were illustrations of results of calculations by the equqtions in the present theory, the increase or the decrease of viscosities of suspensions were described quantitatively without causing a conflict with the existing theories of stractural viscosity.

In addition to the capability of explaining the viscosity change, constant viscosities of agitated suspensions are explainable by the present theory by way of the exsistence of equilibrium between the coagulation rate (H) and the dissociation rate (γ) of particles. By introducing the concept of equilibrium, the reason why many people have been finding constant viscosities of suspensions in the experiments for modifying Einstein's equation[9~13] became explainable.

3.3 Viscosity of unagitated suspensions and the calculation of B_3 and H

For the calculations of time-dependent viscosities and of non-Newtonian flow curves, values of specific constants B_3, H, and U_0 have to be known. Other parameters and conditions such as the primary particle number n_3, the shearing conditions, concentration(s) of dispersant and other auxiliary constituent(s), and the kinds of media are also important, but these are artificially decided.

Although it seems theoretically possible to calculate the coagulation rate constant H from eqs.(7) ~ (17), the calculated values may not be reliable since it is practically impossible to determine the x value (or V_{max}/kT) for the samples of high particle concentrations. The x value calculated from eq. (7) by replacing ϕ by ζ-potential actually determined for the suspension of low particle concentration may not be reliable for describing the property of a thick suspension.

Since it is possible to determine the viscosities of suspensions of various particles concentrations, it seems desirable, if possible, to find the values of specific constants from the actually measured viscosities.

In the present theory, there are several ways of determining the parameters B_3, H, and U_0 from the measured viscosities. Among the methods, there are practical ones which use the viscosity of suspensions left unagitated and another based on the viscosity under a

continuous agitation. The one which uses the viscosity of unagitated suspension is described in this section.

It is possible to calculate B_3 and H from two data points of measured viscosity of a suspension if U_0 value is known, but due to the unavailability of this value and to a relatively low reliability of each single measurement, an application of regression technique was considered desirable.

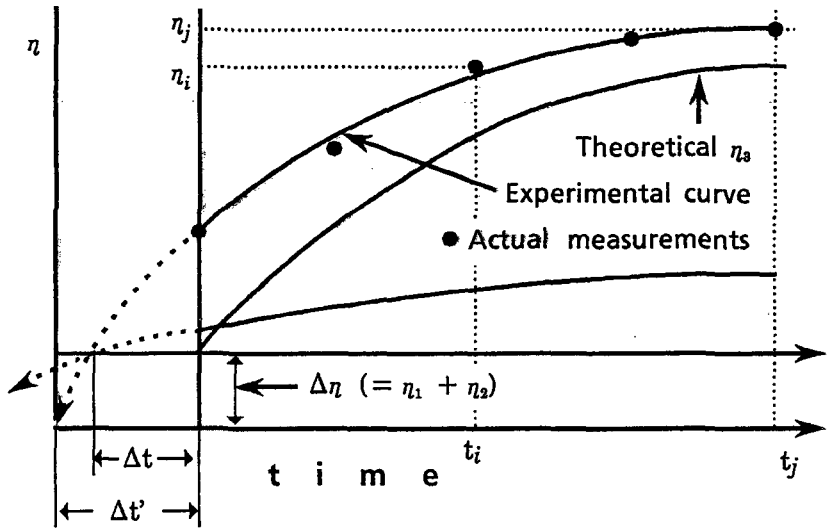

FIGURE 8. Difference between Experimental and Theoretical Curves

For the unagitated condition, the shear rate has to be zero and by assuming that the sample suspension was in the state of complete dispersion ($U_0 = 0$) initially, eq. (26) reduces to;

$$\eta_3^{1.5} = B_3^{1.5} \cdot \frac{n_3 \cdot Ht}{Ht + 1} \qquad \cdots\cdots\cdots\cdots\cdots\cdots (38)$$

For the convenience of employing the technique of linear regression, eq. (38) is transformed as follows;

$$\frac{1}{\eta_3^{1.5}} = \frac{1}{B_3^{1.5} \cdot n_3 \cdot Ht} + \frac{1}{B_3^{1.5} \cdot n_3} \qquad \cdots\cdots\cdots\cdots\cdots\cdots (39)$$

By the use of auxiliary constants E and F where,

$$E = 1/B_3^{1.5} \cdot n_3 \cdot H, \quad \text{and} \quad F = 1/B_3^{1.5} \cdot n_3$$

eq.(39) is furhter transformed as follows;

$$Y = E \cdot X + F \qquad \cdots\cdots\cdots\cdots\cdots\cdots\cdots\cdots\cdots\cdots (40)$$

After obtaining eq.(40) in which $X = 1/t$ and $Y = 1/\eta_3^{1.5}$, the technique of linear regression becomes applicable. Before the regression calculation, it is recommendable to

plot the viscosity data by setting the origin ($t = 0$) at the time of first viscosity measurement, and to estimate the value for $\Delta t'$ by the extrapolation as shown in FIG. 8 by the arrow mark. The estimated value of $\Delta t'$ is used for the first calculation. Although it is desirable to estimate the true value of Δt, it is not possible since there is no way of finding the exact value of $\Delta\eta$ beforehand. It is usually recommendable to use the value equal to 1.3 ~ 2.0 times the viscosity of medium as $\Delta\eta$ depending on the particle concentration.

Since there is an unavoidable difference between the measured data and the theoretical curve as mentioned previously, the corrections for Δt and $\Delta\eta$ are usually required, although the correction for $\Delta\eta$ may be omitted when the lowest measured viscosity is very high (higher than a few hundred times the viscosity of medium). The equations for the corrections of Δt and $\Delta\eta$ are as follows;

$$X_i = 1/(t_i + \Delta t) \quad \cdots\cdots\cdots\cdots\cdots\cdots\cdots\cdots\cdots\cdots (41)$$

$$Y_i = 1/(\eta_i - \Delta\eta)^{1.5} \quad \cdots\cdots\cdots\cdots\cdots\cdots\cdots\cdots\cdots\cdots (42)$$

The measurements of viscosity for the caluculations of B_3 and H have to be done quickly, applying the slowest shear rate possible to minimize the mechanical energy put into the system, since, as defined, eqs. (38), and (39) express the viscosity of unagitated suspensions. A longer time of rotor rotation and a faster shear rate than necessary tend to increase theoretical error and to reduce the reliability of calculated results.

After calculating the values for X_is and Y_is, the constants E and F are calculable as follows;

$$\left.\begin{aligned} \Sigma Y_i &= E\cdot\Sigma X_i + m\cdot F \\ \Sigma X_i\cdot Y_i &= E\cdot\Sigma X_i^2 + F\cdot\Sigma X_i \end{aligned}\right\} \quad \cdots\cdots\cdots\cdots\cdots\cdots (43)$$

m: number of data pairs (X_i, Y_i)

By solving eq. (43), we have,

$$E = (\Sigma X_i\cdot\Sigma Y_i - m\cdot\Sigma X_i\cdot Y_i)/\Delta_0 \quad \cdots\cdots\cdots\cdots\cdots (44)$$

$$F = (\Sigma X_i\cdot\Sigma X_i\cdot Y_i - \Sigma X_i^2\cdot\Sigma Y_i)/\Delta_0 \quad \cdots\cdots\cdots\cdots\cdots\cdots (45)$$

where,

$$\Delta_0 = (\Sigma X_i)^2 - m\cdot\Sigma X_i^2 \quad \cdots\cdots\cdots\cdots\cdots\cdots\cdots\cdots (46)$$

The coefficient of correlation R is,

$$R = \frac{m\cdot\Sigma X_i\cdot Y_i - \Sigma X_i\cdot\Sigma Y_i}{\sqrt{\{(\Sigma X_i)^2 - m\cdot\Sigma X_i^2\}\cdot\{(\Sigma Y_i)^2 - m\cdot\Sigma Y_i^2\}}} \quad \cdots\cdots\cdots (47)$$

If a very smooth curve is obtained by connecting the data points, a very high coefficient of correlation, equal to or higher than 0.99, is usually obtainable, and when the coefficient is very close to 1.0, the data used for the calculation are considered to be mathematically

reliable, although there are causes which may make the difference between the theoretical value and the experimental value larger without degrading the coefficient.

There is a possibility of improving the coefficient of correlation further by adjusting the value for Δt. After maximizing the coefficient R by adjusting Δt, the values for B_3 and H are calculable from E and F as follows;

$$H = F/E \quad \text{.....(48)}$$

$$B_3 = 1/(F \cdot n_3)^{2/3} \quad \text{.....(49)}$$

Not only by adjusting Δt, it is also possible to improve the coefficient of correlation by adjusting $\Delta\eta$, but the effect of $\Delta\eta$ correction is usually smaller than that of Δt and is nearly negligible for the samples of very high viscosity because the ratio $\Delta\eta/\eta_3$ is very low. For this reason, it is not easy to find an accurate value of $\Delta\eta$. FIGs. 9 and 10 and TABLEs 1 and 2 show examples of calculation of specific constants B_3 and H for colloid cement pastes.

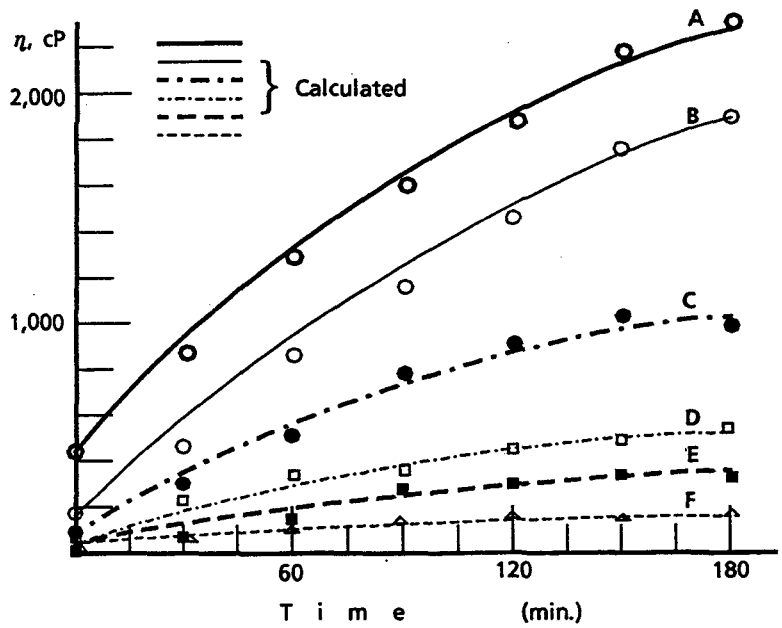

FIGURE 9. Calculation of B_3 and H from Viscosity of Unagitated Cement Pastes

The constsnts and parameters of the paste used for the tests in FIG. 9 and TABLE 1 are as follows;

r	: 1.465 μm	(average radius of cement particle)
n_3	: 1.893 × 10^{10}/cm^3	(primary particle number)
Cv	: 0.241	(volume fraction of cement)
ρ	: 3.15	(specific gravity of cement)
κ	: 2.02 × 10^7	(Debye – Hückel parameter)
I	: 0.37 N/l	(ionic strength)
kT	: 4.045 × 10^{-14}	(at 293 °K)
η_m	: 1.0 cP	(viscosity of water)

TABLE 1 B_3 and H Values Calculated with the Corrections

Sample Dosage*	A 0.0	B 0.4	C 0.6	D 0.8	E 1.0	F 1.2
x	16.34	16.66	17.92	18.56	19.50	20.44
H $\times 10^5$	4.857	3.498	1.000	0.524	0.205	0.081
$B_3 \times 10^6$	6.406	6.008	6.644	6.378	6.663	6.581
Δt, sec.	685	256	320	330	255	318.5
$\Delta\eta$, cP	—	—	—	—	—	1.56

* Dosage of dispersant (formaldehyde high condensate of Na β– naphthalene sulfonate), % by wt. of cement as solid.

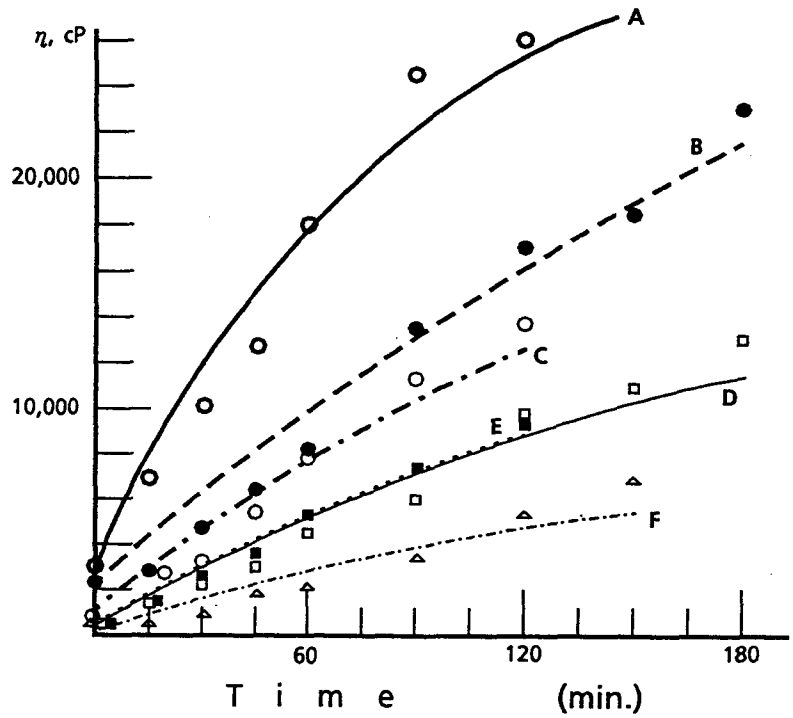

FIGURE 10. Calculation of B_3 and H from Viscosity of Unagitated Cement Pastes

The constsnts and parameters of the paste used for the tests in FIG. 10 and TABLE 2 are;

σ : 6400 cm^2/g (specific surface of cement)
r : 1.552 μm
ρ : 3.15 (specific gravity of cement)

W/C : 0.6, 0.7, 0.8
Cv : 0.3556, 0.32113 0.29274
n_3 : 2.271 2.0508 1.8695 ($\times 10^{10}$)

TABLE 2. Specific Constants of Colloid Cement

	A	B	C	D	E	F
W/C	0.6		0.7		0.8	
Disp.*	0.25	0.40	0.25	0.40	0.25	0.40
Time (min.)	Viscosity (cP)					
0	3000	2250	750	575	600	475
15	7000	2800	2750	1525	1640	730
30	10150	4600	3250	2200	2560	1250
45	12650	6200	5750	3000	3650	1890
60	18000	8200	8000	4650	5250	2200
90	24500	13500	11250	6000	7200	3600
120	26000	17200	13750	9700	9500	5200
150		18300		11200		6600
180		23000		13000		7200
$B_3 \times 10^4$	7.955	8.049	8.409	8.885	16.760	8.157
$H \times 10^6$	10.080	2.801	2.760	1.159	0.5633	0.5143
R**	0.9994	0.9554	0.9990	0.9983	0.9986	0.9768
Δt (sec.)	318.6	668.0	148.6	217.3	202.3	439.3

* Dosage of dispersant (β– NS), % by wt. of Cement as solid.
** Coefficient of correlation

After H and Δt are calculated, U_0 becomes calculable as follows ;

$$U_0 = H \cdot \Delta t / (H \cdot \Delta t + 1) \quad \ldots\ldots\ldots\ldots\ldots\ldots\ldots\ldots (50)$$

As explained previously, it is important to minimize the energy of agitation put into the system of viscosity measurements for improving the reliability of calculated results. Other than the energy of agitation, quick response of a viscometer in indicating correct values of viscosity is very important since the time lag between the instant of starting rotor rotation and the time at which the reading on the indicator reaches the maximum causes an error in the time–viscosity record of the measurements.

The viscosity of unagitated suspension increases continuously as shown by A in FIG. 11, but it turns to decrease at the time when the rotor rotation is started as shown by the broken line B. Due to the influence of inertia of the rotor and of the sample fluid, it takes a while for the rotor to move at a predetermined speed (shear rate). The reading of viscometer continuously increases as shown by the arrows on the curves but the true viscosity decreases during this period.

As described in this section, the specific constants B_3, H, and U_0 are calculable from viscosities of a suspension left unagitated, but due to the energy supplyed to the system by the rotor rotation,a certain extent of error as shown by the curves A, B, and C in FIG. 11 is unavoidable.

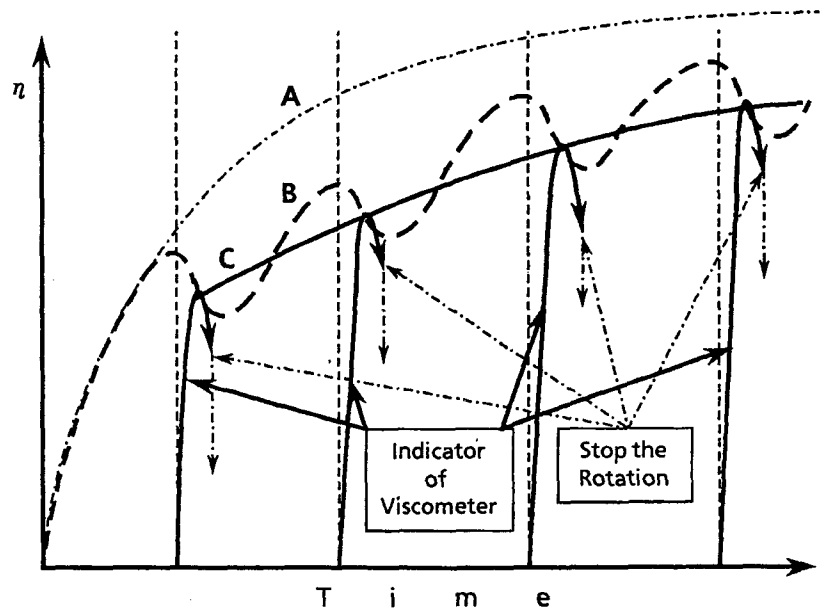

FIGURE 11. Curve s for Actual Viscosity and Calculated Viscosity

3.4 Viscosity of suspensions continuously agitated and the calculation of B_3 and H

Same as the procedure of calculation of specific constants B_3 and H based on eq. (13), the constants are calculable from the decreasing viscosity under a constant agitation (shear rate) by neglecting the coagulation rate constant H. By experiences, it has been known that the H values of many suspensions are in the range between 10^{-3} and 10^{-9}, and the shear rate (γ) attainable by popularly used rotational viscometers are in the range between 10^{-1} and 10^{3}. Due to the fact that the value for shear rate is usually much larger than the value for H, less influence of the neglect of H than of γ is expected, and accordingly, the better results of calculation are expected by the procedure based on eq. (27) expressing the decreasing viscosity under a constant shear rate.

From eq. (27) with the neglect of H, we have,

$$\eta_s = B_3 \cdot \left\{ \frac{n_3}{\gamma t + 1} \right\}^{2/3} \qquad \cdots\cdots\cdots\cdots\cdots\cdots\cdots\cdots (51)$$

As shown by FIG. 12, the viscosity of sample follows the curve for eq. (27) if a constant shear rate is applied, and the curves for eqs. (27) and (51) agree very closely if the time of

viscossity measurements (t_a and t_b) are considerably shorter than the time of equilibrium

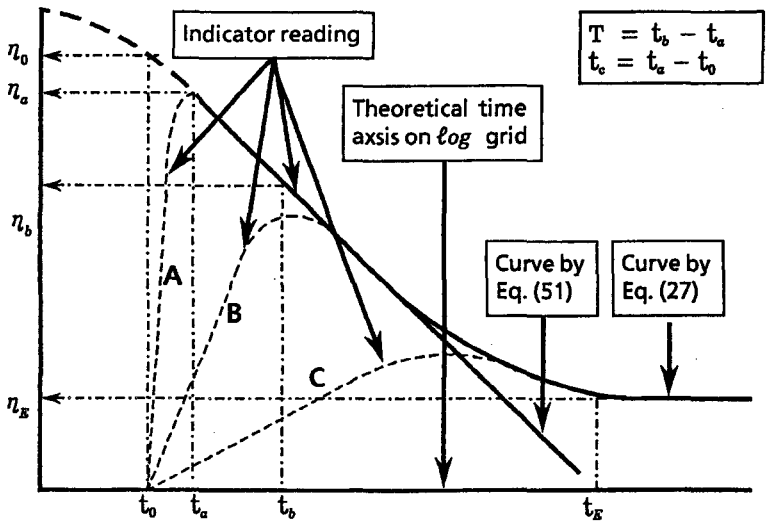

FIGURE 12. Calculation of B_3 and H from Decreasing Viscosity

(t_E). From the measurement under a constant shear rate, η_a, η_b, η_E, T which is the interval between t_a and t_b, and t_c which is the interval between t_0 and t_a are known. If an accurate value of t_E is known by an experiment, H value is easily calculable by eq. (32) from the shear rate, but it is usually difficult to determine the time of equilibrium t_E accurately because the rate of viscosity decrease is very small in the neighbourhood of equilibrium and there is no sharp inflection point on the time–viscosity curve.

The theoretical error caused by the use of eq. (51) instead of (27) may be estimated as follows. Obviously, the error is not caused if (H·t + 1) is equal to 1. To limit the error within several per cent, H·t has to be less than about 0.05, so the available time for the viscosity measurement is,

$$t \leqq 0.05/H \qquad \text{.....(52)}$$

From eq. (52), it is known that the measurement of viscosity is easier for the samples of smaller H since the available time for the measurement is longer. From the results of measurement, we have,

$$\left.\begin{aligned} \eta_a^{1.5} &= \frac{B_3^{1.5}\cdot n_3}{\gamma t_a + 1} \\ \eta_b^{1.5} &= \frac{B_3^{1.5}\cdot n_3}{\gamma t_b + 1} \end{aligned}\right\} \qquad \text{.....(53)}$$

and from eq. (53), we can calculate R as follows;

$$R = \frac{\eta_a^{1.5}}{\eta_b^{1.5}} = \frac{\gamma \cdot t_b + 1}{\gamma \cdot t_a + 1} \qquad \cdots\cdots(54)$$

$$R \cdot (\gamma \cdot t_a + 1) = \gamma \cdot t_b + 1 = \gamma \cdot (t_a + T) + 1 \qquad \cdots\cdots(55)$$

Since all the values except for t_a in eq. (55) are known, it is calculable as follows;

$$t_a = \frac{\gamma \cdot T + 1 - R}{\gamma \cdot (R - 1)} \qquad \cdots\cdots(56)$$

After calculating t_a, the initial time t_0 on the theoretical time axis and U_0 are calculable as follows;

$$t_0 = t_a - t_c, \quad U_0 = 1/(\gamma \cdot t_0 + 1)$$

The B_3 value is calculable by subsituting the value t_a or t_b which is equal to $(t_a + T)$ into eq. (53), and finally H value is calculable from U_E by using eq. (34) as follows;

$$\eta_E^{1.5} = B_3^{1.5} \cdot n_3 \left\{ \frac{2 \cdot \sqrt{\gamma \cdot H} + H}{(\sqrt{H} + \sqrt{\gamma})^2} \right\} \qquad \cdots\cdots(34')$$

$$H \cdot (1 - U_E) + 2\sqrt{\gamma H} \cdot (1 - U_E) - \gamma \cdot U_E = 0 \qquad \cdots\cdots(57)$$

From (57), we have,

$$\sqrt{H} = \frac{\sqrt{\gamma} \cdot \{\sqrt{1 - U_E} - (1 - U_E)\}}{(1 - U_E)}$$

and,

$$H = \frac{\gamma \cdot \{2 - U_E - 2\sqrt{(1 - U_E)}\}}{(1 - U_E)} \qquad \cdots\cdots(58)$$

Due to the neglect of H instead of γ which is usually much larger than H, the procedure of calculation of B_3 and H from decreasing viscosities described above is expected to be more reliable than the previous one, but the same problem caused by the poor response or the time–lag of the viscometer exsists. If the time–lag is short enough, the indicator displays the data following the curves **A** or **B** in FIG 12, and the values of B_3 and H calculated from these data are considered to be fairly reliable, but as shown by the curve **C**, the viscosity indicated by a viscometer of very poor response does not agree with that calculated by eq. (51).

Another problem associated with the procedures of calculation of B_3 and H from the measured viscosities is the accuracy of shear rate. Depending on the mechanical structure of viscometers, the extent of error caused by the end effect included in the results of measuements is different. Although the results obtained for a Newtonian fluid by the viscometers of different end effects are identical, the results for a non–Newtonian fluid are, in some cases, entirely different. The viscometer the shear rate of which is calibrated by using a Newtonian fluid of known viscosity are usually unsatisfactory for the measurements of non–Newtonian viscosities.

Some examples of calculation by the procedure described above is shown below. The constants and parameters used for the calculations are as follows;

Table 3 Calculation of Specific Constants from Decreasing Viscosity

Test	A	B	C	D
Rotor Speed (rpm)	10.06	12.10	14.20	14.20
γ	19.42	23.35	27.406	27.406
β–NS	1.0	1.25	1.5	1.5
η_a (P)	100.13	66.36	96.866	90.685
η_b (P)	87.77	60.41	90.685	77.585
η_E (P)	51.49	38.12	24.908	24.908
η_{max} (P)	5838.40	5582.43	11644.8	5861.78
T (sec)	5	5	5	5
R	1.2185	1.1513	1.104	1.2637
t_a (sec)	22.88	33.00	48.05	18.93
$B_3 \times 10^3$	1.14	1.09	2.274	1.144
$H \times 10^6$	3.33	1.86	0.067	0.5244
t_E (sec)	124.29	151.74	737.74	263.78

r : radius of particle, 2.261 μm
Cv : particle concentration, 0.561
W/C : water/cement ratio, 0.25
n_3 : primary particle number, $1.159 \times 10^{10}/cm^3$
Dispersant : β–NS, 1.0 ~ 1.5 % by weight of cement

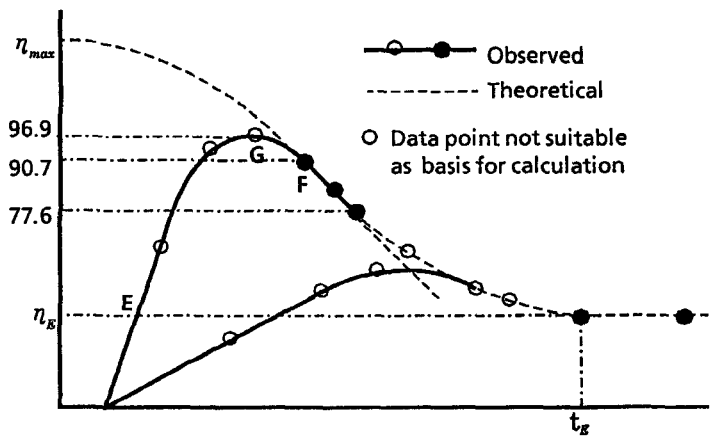

FIGURE 12'. Selection of Data Point for Calculations of B_3 and H

By the present theory, viscosity (η_{max}) at the state of complete coagulation and B_3 value have to be the same for samples of the same particle concentration in the same kind of medium. All results of B_3 and η_{max} calculations except for test C in TABLE 3 were in a good agreement. The H value decreased according to the increase in the dosages of dispersant. Since the data points for tests C and D were selected from one experiment (curve E in FIG. 12'), the reason of obtaining an exceptional result of calculation in test C may be attributable to the selection of data point G in FIG. 12' instead of F as η_a.

4. Extension of Newton's law and calculation of flow curves

4.1 Extension of Newton's flow equation to non–Newtonian fluids

After the Newtonian and the non–Newtonian viscosities were explained by the same mechanism and the non–Newtonian viscosity was described as functions of time and the shear rate, the flow equation for Newtonian fluids (1) was extended to non–Newtinian fluids as shown by eq. (5) previously. After the extension expressed by eq. (5) and derivations of practical viscosity equations (26) ~ (31) and of shear rate equations (37.1) ~ (37.9), the following flow equation in differential form became meaningful for the examination and for the prediction of non–Newtonian flow curves.

$$\frac{d\tau}{dt} = \frac{d(\eta_s \cdot \gamma)}{dt} = \eta_s \frac{d\gamma}{dt} + \gamma \frac{d\eta_s}{dt}$$

$$= (\eta_1 + \eta_2 + \eta_3)\cdot\frac{d\gamma}{dt} + \gamma \frac{d\eta_3}{dt} \qquad \cdots\cdots\cdots\cdots\cdots\cdots (59)$$

Since the shapes of flow curves on (τ, γ) plane agree with those on (τ, t) plane when the shear rate is proportional to the time, the shapes of flow curves are mathematically predictable by calculating the time–dependency of $d\tau/dt$. For the calculation of $d\tau/dt$, the practical forms of equations expressing η_3 and γ and the derivatives thereof have to be known. The $d\gamma/dt$ are easily calculable from eqs. (37.3) ~ (37.9) but $d\eta_3/dt$ for the equations containing the terms $G\cdot t^{\alpha}$ or $G\cdot(T - t)^{\alpha}$ are fairly complicated. For the convenience of calculation by eq. (59), two sets of equations were calculated as follows;

Set A

$$\gamma = G\cdot t^{\alpha} \qquad \cdots\cdots\cdots\cdots\cdots\cdots (37.4)$$

$$d\gamma/dt = \alpha\cdot G\cdot t^{(\alpha-1)} \qquad \cdots\cdots\cdots\cdots\cdots\cdots (60)$$

$$\eta_3 = B_3\cdot n_3^{2/3}\cdot\left\{\frac{U_a\cdot(GHt^{(\alpha+2)} + 1) + Ht}{(Ht + 1)(Gt^{(\alpha+1)} + 1)}\right\}^{2/3} \qquad \cdots\cdots\cdots\cdots (26.1)$$

$$\frac{d\eta_3}{dt} = \frac{2\cdot B_3\cdot n_3^{2/3}}{3}\cdot\left\{\frac{(G\cdot t^{(\alpha+1)} + 1)\cdot(Ht + 1)}{U_a(GHt^{(\alpha+2)} + 1) + Ht}\right\}^{1/3}$$

$$\cdot\frac{G\cdot t^{\alpha}\cdot[(\alpha + 1)\cdot\{U_a(H^2t^2 - 1) - H^2t^2\} + Ht\cdot(U_a\cdot G\cdot t^{(\alpha+1)} - \alpha)] + (1 - U_a)\cdot H}{(G\cdot t^{(\alpha+1)} + 1)^2\cdot(Ht + 1)^2}$$

$$\cdots\cdots\cdots\cdots\cdots\cdots (61)$$

Set B

$$\gamma = G\cdot(T - t)^{\alpha}, \quad T/2 \leqq t \leqq T \qquad \cdots\cdots\cdots\cdots\cdots\cdots (37.6)$$

$$d\gamma/dt = -\alpha\cdot G\cdot(T - t)^{(\alpha-1)} \qquad \cdots\cdots\cdots\cdots\cdots\cdots (62)$$

$$\eta_3 = B_3 n_3^{2/3}\cdot\left\{\frac{U_b\cdot(GHt^2\cdot(T - t)^{\alpha} + 1) + Ht}{(Ht + 1)\cdot\{G\cdot(T - t)^{\alpha}\cdot t + 1\}}\right\}^{2/3} \qquad \cdots\cdots\cdots\cdots (26.2)$$

$$\frac{d\eta_3}{dt} = \frac{2\cdot B_3\cdot n_3^{2/3}}{3}\cdot\left[\frac{(Ht+1)\cdot\{G\cdot(T-t)^a\cdot t+1\}}{U_b\cdot(GHt^2\cdot(T-t)^a+1)+Ht}\right]^{1/3}\cdot$$

$$\frac{G\cdot(T-t)^{(a-1)}[GHt^2U_b(T-t)^{(a+1)}+\{T-(a+1)t\}\cdot\{U_b(H^2t^2-1)-H^2t^2\}+aHt^2]+(1-U_b)H}{(Ht+1)^2\cdot\{Gt\cdot(T-t)^a+1\}^2}$$

.....(63)

Although two sets of equations A and B shown above are useful for the examinations of flow curves and hysteresis, these may be too complicated for the calculation practices. For the purpose of examining the theoretical influences of coagulation rate constant H or the shearing condition G on the shape of flow curves, it is not necessary to use general equations containing the initial conditions (U_a and U_b) and wide variety of shearing conditions. For this purpose, simpler equations such as (27), (37.3), and (27.1) are considered satisfactory.

If a is equal to 1, equations in the above sets are simplified as follows;

Set C

$$\gamma = G\cdot t \qquad \text{.....(37.3)}$$

$$d\gamma/dt = G \qquad \text{.....(64)}$$

$$\eta_3 = B_3\cdot n_3^{2/3}\cdot\left\{\frac{U_a\cdot(GHt^3+1)+Ht}{(Ht+1)(Gt^2+1)}\right\}^{2/3} \qquad \text{.....(26.3)}$$

$$\frac{d\eta_3}{dt} = \frac{2\cdot B_3\cdot n_3^{2/3}}{3}\cdot\left\{\frac{(G\cdot t^2+1)\cdot(Ht+1)}{U_a(GHt^3+1)+Ht}\right\}^{1/3}$$

$$\frac{G\cdot t\cdot(U_aGHt^3-Ht-2U_a)+H\cdot(2GHt^3-1)\cdot(U_a-1)}{(G\cdot t^2+1)^2\cdot(Ht+1)^2}$$

.....(65)

Set D

$$\gamma = G\cdot(T-t), \qquad T/2 \leqq t \leqq T \qquad \text{.....(37.5)}$$

$$d\gamma/dt = -G \qquad \text{.....(66)}$$

$$\eta_3 = B_3\cdot n_3^{2/3}\cdot\left\{\frac{U_b\cdot(GHt^2\cdot(T-t)+1)+Ht}{(Ht+1)\cdot\{G\cdot(T-t)\cdot t+1\}}\right\}^{2/3} \qquad \text{.....(67)}$$

$$\frac{d\eta_3}{dt} = \frac{2\cdot B_3\cdot n_3^{2/3}}{3}\cdot\left[\frac{(Ht+1)\cdot\{G\cdot(T-t)\cdot t+1\}}{U_b\cdot(GHt^2\cdot(T-t)+1)+Ht}\right]^{1/3}\cdot$$

$$\frac{G\cdot[GHt^2U_b(T-t)^2+(T-2\cdot t)\cdot\{U_b(H^2t^2-1)-H^2t^2\}+Ht^2]+(1-U_b)H}{(Ht+1)^2\cdot\{Gt\cdot(T-t)^2+1\}^2}$$

.....(68)

Equations (26.3) and (65) are further simplified if the shear rate is increased proportionally to the time and the suspension sample is initially in the state of complete coagulation.

Set E

$$\gamma = G{\cdot}t \qquad \cdots\cdots(37.3)$$

$$d\gamma/dt = G \qquad \cdots\cdots(69)$$

$$\eta_3 = B_3{\cdot}n_3^{2/3}{\cdot}\left\{1 - \frac{G{\cdot}t^2}{(H{\cdot}t + 1)(G{\cdot}t^2 + 1)}\right\}^{2/3} \qquad \cdots\cdots(27.1)$$

$$\frac{d\eta_3}{dt} = \frac{2{\cdot}B_3{\cdot}n_3^{2/3}}{3}{\cdot}\left\{\frac{(G{\cdot}t^2 + 1){\cdot}(H{\cdot}t + 1)}{GHt^3 + H{\cdot}t + 1}\right\}^{1/3}{\cdot}\frac{Gt{\cdot}(GHt^3 - Ht - 2)}{(Gt^2 + 1)^2(Ht + 1)^2}$$

$$\cdots\cdots(70)$$

In contrast to eq. (65), eqs. (67) and (68) in **sets B** and **D** for the calculations of down curves of hysteresiss loops must not be simplified further, because the sspensions are not in the state of complete coagulation nor in the state of complete dispersion at the turning poimt ($t = T/2$) where the shear rate turns to decrease. By the use of any set of equations shown as above, the curves describing the relationship between $d\tau/dt$ and the time are calculable and from the $d\tau/dt$ curves, the properties of non–Newtonian flow curves of suspensions become predictable.

For expressing the relationship between the shear stress and the shear rate directly, eq. (59) may be transformed as follows;

$$\frac{d\tau}{d\gamma} = \eta_1 + \eta_2 + \eta_3 + \gamma\frac{d\eta_3}{d\gamma} \qquad \cdots\cdots(71)$$

but the calculations of whole flow curves by eq. (71) are complicated as shown by the following **sets F** and **G** and are not suitable for the practices except for the calculations of rheology parameters (yield stress τ_0, and Bingham's plastic viscosity $d\tau/d\gamma$) by eq. (72).

$$\tau_0 = \tau_c - \frac{\gamma_c d\tau_c}{d\gamma_c} \qquad \cdots\cdots(72)$$

Set F

$$\gamma = G{\cdot}t \qquad \cdots\cdots(37.3)$$

$$dt/d\gamma = 1/G \qquad \cdots\cdots(73)$$

$$\eta_3 = B_3{\cdot}n_3^{2/3}{\cdot}\left\{\frac{U_a{\cdot}(H\gamma^3 + G^2) + GH\gamma}{(H\gamma + G){\cdot}(\gamma^2 + G)}\right\}^{2/3} \qquad \cdots\cdots(74)$$

$$\frac{d\eta_3}{d\gamma} = \frac{2{\cdot}B_3{\cdot}n_3^{2/3}}{3}{\cdot}\left\{\frac{(\gamma^2 + G){\cdot}(H\gamma + G)}{U_a(H\gamma^3 + G^2) + GH\gamma}\right\}^{1/3}{\cdot}$$

$$\frac{G{\cdot}\{\gamma{\cdot}(U_a\gamma^3H - G\gamma H - 2U_aG^2) + H{\cdot}(2\gamma^3H - G^2){\cdot}(U_a - 1)\}}{(H\gamma + G)^2{\cdot}(\gamma^2 + G)^2}$$

$$\cdots\cdots(75)$$

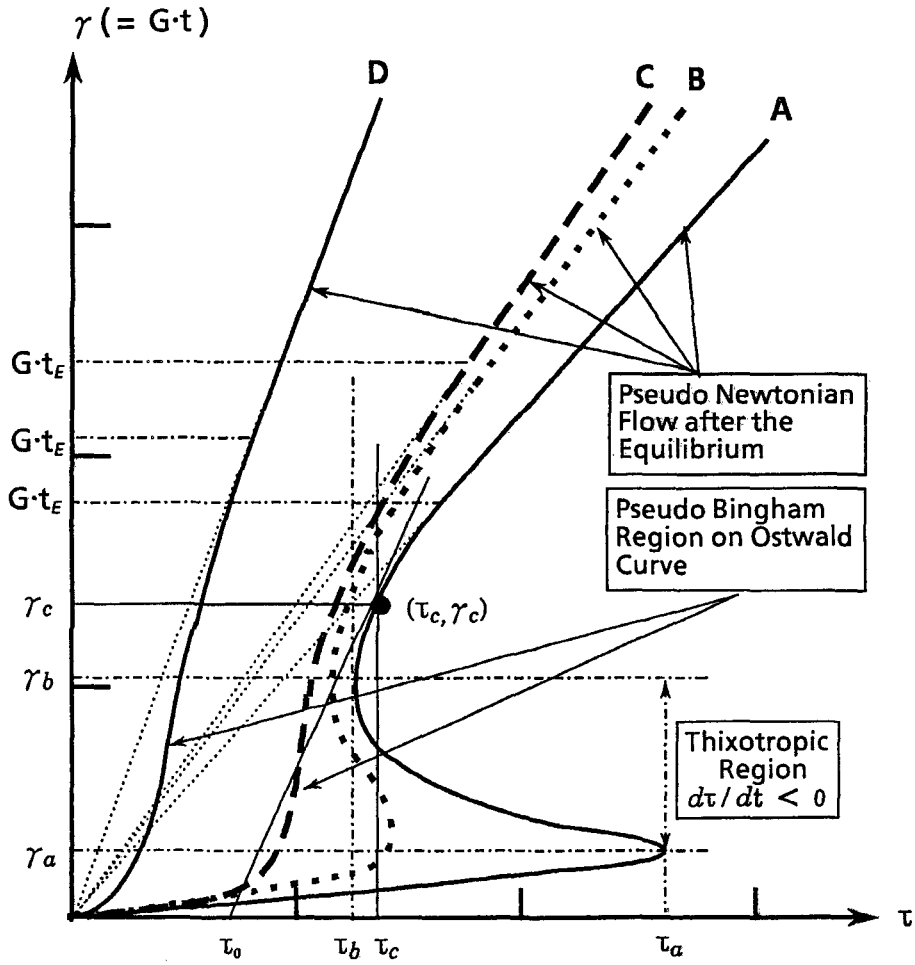

FIGURE 13 Typical flow curves of suspensions

Set G

$$\gamma = G \cdot t^{a} \longrightarrow\longrightarrow t = (\gamma/G)^{1/a} \quad \cdots\cdots\cdots\cdots\cdots\cdots\cdots\cdots (76)$$

by writing $\omega = 1/a$

$$dt/d\gamma = \omega \cdot \gamma^{(\omega - 1)} / G^{\omega} \quad \cdots\cdots\cdots\cdots\cdots\cdots\cdots\cdots (77)$$

$$\eta_s = B_3 \cdot n_3^{2/3} \cdot \left\{ \frac{U_a \cdot (H\gamma^{(1+2\omega)} + G^{2\omega}) + HG^{\omega}\gamma^{\omega}}{(H\gamma^{\omega} + G^{\omega}) \cdot (\gamma^{(1+\omega)} + G^{\omega})} \right\}^{2/3} \quad \cdots\cdots\cdots\cdots (78)$$

$$\frac{d\eta_s}{d\gamma} = \frac{2\cdot B_3\cdot n_3^{2/3}}{3}\cdot\left\{\frac{(\gamma^{(1+\omega)} + G^{\omega})\cdot(H\gamma^{\omega} + G^{\omega})}{U_a(H\gamma^{(1+2\omega)} + G^{2\omega}) + HG^{\omega}\gamma^{\omega}}\right\}^{1/3}\cdot$$

$$\frac{(1+\omega)\cdot G^{\omega}\gamma^{\omega}\cdot\{(U_a-1)\cdot H^2\cdot\gamma^{2\omega} - U_a G^{2\omega}\} + \omega H\cdot G^{\omega}\{U_a\gamma^{(1+3\omega)} - (U_a-1)G^{2\omega}\gamma^{(\omega-1)}\} - HG^{2\omega}\gamma^{2\omega}}{(H\gamma^{\omega} + G^{\omega})^2\cdot(\gamma^{(1+\omega)} + G^{\omega})^2} \quad \cdots\cdots(79)$$

After the extension of Newton's flow equation to non–Newtonian fluids, flow curves and hysteresis loops became calculable, and the meanings of rheological parameters (τ_0 and plastic viscosity) became calculable and explainable on the same basis as Newtonian fluids.

4.2 Influence of experimental conditions U_0 and G on the shape of flow curve

The shapes of flow curves are influenced by the test conditions (U_0 and G) and by the property of suspension samples (H). Immediately after the vigorous agitation for mixing the particles and the medium, U_0 takes a low value and it increases and approaches 1 during the unagitated period before starting the experiments. The longer the standing time before the experiment, the larger the U_0 value which makes the range of variation of $d\tau/dt$ wider.

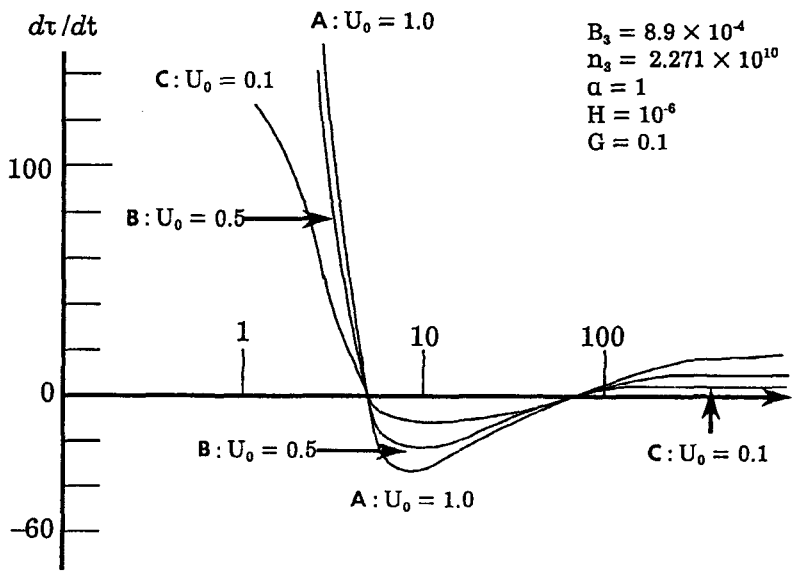

FIGURE 14 Influence of initial viscosity on dτ/dt

As is obvious from the equations expressing $d\tau$ / dt previously shown, τ increases according to the increase in γ when $d\tau/dt$ is positive. When the $d\tau$ / dt curve passes through the negative region, there appears a so called thixotoropic region on the flow curve. So the decrease in U_0 value causes the change in the shapes of flow curves from A to B as shown in FIG. 13. The influence of U_0 on a $d\tau/dt$ curve is shown as follows by FIG. 14.

Other than the influence of U_0 value, the shapes of flow curves are also influenced by the shearing condition G. The influence of G is directionally the same as that of U_0, that is, the larger the G value, the wider the range of variation of $d\tau/dt$. The decrease in G value causes a variation in the shapes of flow curves from A to D as shown in FIG. 13. The influence of G on $d\tau/dt$ is shown in FIG. 15. As shown by eqs. (37.1) ~ (37.9), the shearing condition is not solely represented by G, and $d\tau/dt$ varies according to the change of parameters α and ω.

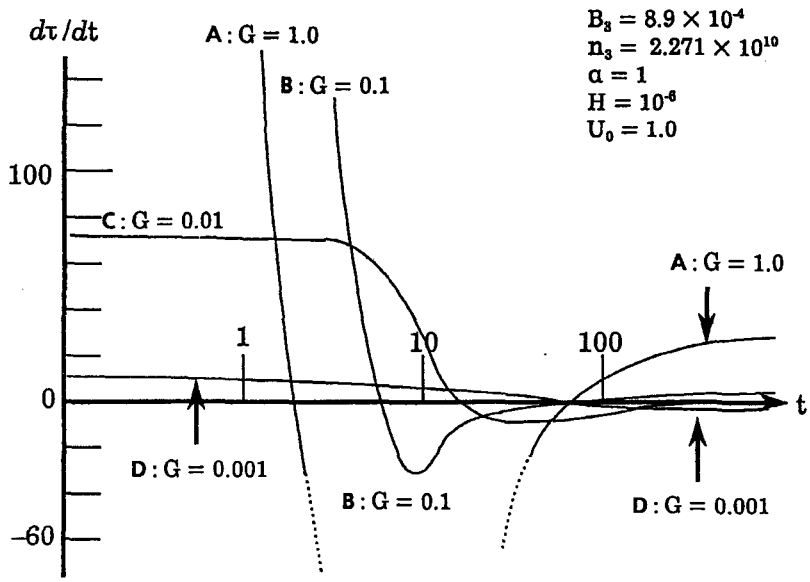

FIGURE 15 Influence of shearing condition G on dτ/dt

4.3 Influence of coagulation rate H on the $d\tau/dt$ curve

FIG. 16 shows the influence of coagulation rate constant H on the shape of $d\tau/dt$ curve. The decrease in H value causes the changes of flow curves from D to A as shown in FIG. 13.

Among the parameters causing changes in the shapes of flow curves, H is only one which is closely related to the chemical composition of suspensions. Addition of dispersant or the use of viscous medium usually cause a decrease and a higher particle concentration or a larger number of primary particle tend to cause an increase in H value, but it is difficult to predict an exact figure before the flow curve experiments.

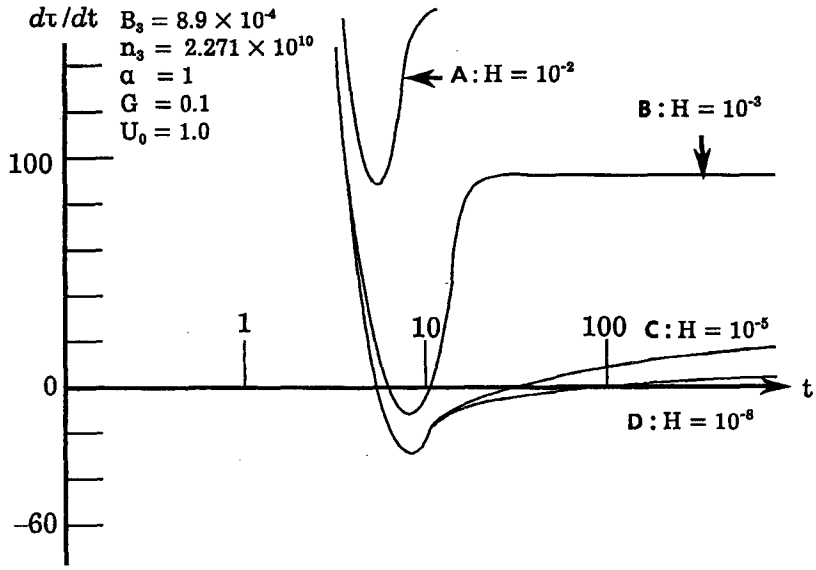

FIGURE 16 Influence of coagulation rate constant H on $d\tau/dt$

Mild agitation during the sample preparation, the longer unagitated time before the rheological experiment, and the larger H value tend to cause an increase in U_0 value, but same as the H value, it is practically impossible to predict an exact figure before the experiments. Since U_0 and H are predictable and controllable only directionally, G (or γ) is the only parameter which is fully controllable artificially and this is the reason why the flow curves and hysteresisloops are unrepeatable.

Since not all factors causing variations in the shapes of flow curves are fully controllable, it is meaningless to classify the fluids as substance by the shape of flow curves, although it may not be meaningless to classify them as phenomena. Although the shapes of flow curves or the flow properties of suspensions are not fully controllable, the direction of transition from a flow type to another is explainable and predictable by the calculation of $d\tau/dt$ or $d\tau/d\gamma$ as described in this chaptor.

LITERATURE

1) Florian Cajori, "PRINCIPIA", – The Revision of translation of Sir Isaac Newton's "Mathematical Principles of Natural Philosophy" by Andrew Motte in 1729, Vol. I, Section 9, 'The Circular Motion of Fluids' p. 385, (1971), Univ. of California Press, Berkeley, Los Angeles, London
2) G. Hagen, Pogg. Ann., 46, 437, (1839)
3) J. Poiseuille, Ann. Chim. Phys., [3], 7, 50, (1843)
4) E. C. Bingham, US Bureau of Std. Bulletin, 13, 309, (1916)
5) E. C. Bingham, "Fluidity and Plasticity", p. 203, (1922), McGraw Hill, New York
6) W. H. Herschel, R. Bulkley, J. Phys. Chem., 29, 1217, (1925)
7) W. H. Herschel, R. Bulkley, Proc. Annual Meeting of ASTM, 26, II, p. 621, June 21 ~ 25, (1926), Atlantic City, NJ
8) N. Casson, "Rheology of Disperse Systems", ed. by C. C. Mill, p. 84, (1959)
9) A. Einstein, Annalen Phys. 9, 289 ~ 306, (1906)
10) A. Einstein, Annalen Phys. 34, 581, (1911)
11) Ir. R. Rutgers, Rheol. Acta, 2, (3), 202 ~ 210, (1962)
12) Ibid., 2, (4), 305 ~ 348, (1962)
13) Ibid., 3, (2), 118 ~ 122, (1963)
14) C. F. Goodeve, Trans. Faraday Soc., 35, 342, (1939)
15) C. F. Goodeve, G. W. Whitfield, Trans. Faraday Soc., 34, 511, (1938)
16) R. V. Williamson, Ind. Eng. Chem., 21, 1108, (1929)
17) T. Gillespie, Rheol. Abstr., 5, (3), 34, (1962)
18) T. Gillespie, J. Colloid Sci., 15, 219, (1960)
19) T. Gillespie, J. Polym. Sci., 46, 383, (1960)
20) T. Gillespie, Trans. Soc. Rheol., (2), 35, (1965)
21) T. Gillespie, J. Colloid Interface Sci., 22, 554 ~ 562, (1966)
22) T. Gillespie, J. Colloid Interface Sci., 22, 563 ~ 572, (1966)
23) B. T. Storey, E. W. Merrill, J. Polym. Sci., 33, 361, (1958)
24) G. W. Scott Blair, Rheol. Acta, 4, 53, (1965)
25) G. W. Scott Blair, Rheol. Acta, 4, 152, (1965)
26) G. W. Scott Blair, Rheol. Acta, 6, 201, (1967)
27) G. W. Scott Blair, "Elementary Rheology", p. 50 ~ 58, (1969) Academic Press, London, New York
28) S. Oka, J. Applied Phys. (Japan) 40, (1), 105, (1971)
29) S. Oka, "Rheology –Biorheology–", 2nd ed. p. 19, (1976) Shokabou, Tokyo
30) K. Hattori, K. Izumi, J. Dispersion Sci. Tech., Part 1, 3, (2), 129, (1982)
31) Part 2, Ibid., 3, (2), 147, (1982)
32) Part 3, Ibid., 3, (2), 169, (1982)
33) Part 4, Ibid., 11, (3) 307, (1990)
34) K. Hattori, K. Izumi, "Proc. Symposium M, Annual Meeting of Materials Res. Soc.", p. 14, (1982), Edited by J. P. Skalney: Nov. 1 ~ 4, Boston Mass.
35) K. Hattori, K. Izumi, J. Materials Sci. (Japan), 32, (356), 461, (1983)

36) K. Hattori, K. Izumi, Ceramics, (Japan), 18, (2), 103, (1983)

37) H. Fujiwara, K. Izumi, et. al., Proc. International Symposium on Wood and Pulping Chem., Vol. III, p. 95, May 23 ~ 27, (1983), Tsukuba Science City, Ibaraki,

38) E. J. W. Verwey, J. Th. G. Overbeek, "Theory of the Stability of Lyophobic Colloids", (1948), Elsvier Publishing Co., Ltd.

39) G. H. Tattersall, Brit. J. Appl. Phys., 6, 165, (1955)

40) G. H. Tattersall, Nature, 175, 166, (1955)

41) K. Hattori, K. Izumi, "Second International Conference on the Use of Fly Ash, Silica Fume, Slag and Natural Pozzolans in Concrete", 21 ~ 25, April, (1986),
Madrid, Spain